Available online at www.sciencedirect.com
ScienceDirect
Trans. Nonferrous Met. Soc. China 31(2021) 1165−1174
Transactions of Nonferrous Metals Society of China
www.tnmsc.cn

Thermodynamic simulation of complex Pb−Bi concentrate oxidative bath smelting process

Lin CHEN[1,2], Peng CHEN[1,2], Du-chao ZHANG[1,2], Wei-feng LIU[1,2], Tian-zu YANG[1,2]

1. School of Metallurgy and Environment, Central South University, Changsha 410083, China;
2. National Engineering Laboratory for High Efficiency Recovery of Refractory Nonferrous Metals, Central South University, Changsha 410083, China

Received 30 April 2020; accepted 28 October 2020

Abstract: The element partitioning in a Pb−Bi concentrate oxygen-rich bath smelting process was studied using thermodynamic equilibrium simulation method. Effects of oxygen to feed ratio (OFR) and sulfur dioxide partial pressure (p_{SO_2}) on the partitionings of Bi, Pb, As, Sb, Cu and Ag were analyzed and compared with industrial data. The results suggested that the optimal OFR was between 6.3 and 6.8 kmol/t to maximize Bi, Pb, Cu and Ag partitioning in the metal phase. Further increase of OFR led to the drop of metal partitioning and increase of slag liquidus temperature. High p_{SO_2} led to high deportment of Bi and Pb in the gas phase mainly in the form of sulfides, suggesting that a low p_{SO_2} was conducive for reducing the dust ratio.

Key words: complex Pb−Bi concentrate; oxygen-rich bath smelting; multiphase equilibrium simulation; element partitioning; process parameter optimization

1 Introduction

From last decade, the non-ferrous metallurgical industry has witnessed an evolution of the pyrometallurgical methods during which the traditional blast furnace and reverberatory smelting technologies were substituted by oxygen-rich bath smelting technologies for processing the concentrates [1,2], complex minerals [3] and secondary resources [4]. Compared with the traditional processes, the bath smelting technologies not only have higher capacity and metal recovery but also are more energy efficient and environmental-friendly [5]. Efforts were devoted to the thermodynamics [6], hydraulics [7] and new energy resources [8], and the behaviors of minor elements have become a recent focus due to their continuous rising grade in the raw materials [9].

Bi has a geochemical abundance of only 2×10^{-7} and shows important applications in the medical, chemical engineering and electronic industries [10,11]. The traditional pyrometallurgical techniques for the smelting of Bi concentrate are precipitation smelting, oxidative smelting or a combination of these two smelting processes in a blast furnace or reverberatory furnace. The processes suffer from high energy consumption as well as environmental pollution caused by the by-product, i.e. flue gas with low SO_2 contents and low-grade matte [12]. As environmental regulations are becoming stricter, it is urgent to develop an efficient method for processing complex Bi resources with less environmental footprint. YANG et al [13] proposed a process in which Bi concentrate was first smelted to produce oxidized slag, and then the slag was reduced to produce Bi ingot. The process was commercialized using two

Corresponding author: Du-chao ZHANG; Tel: +86-13787003744; E-mail: zdc015@sina.com
DOI: 10.1016/S1003-6326(21)65569-3

oxygen-rich side blow bath smelting furnaces (OSBFs), which greatly raised metal recovery and reduced energy consumption. Moreover, the flue gas had a high SO_2 content, which facilitated its utilization for H_2SO_4 production [14]. However, the contents of minor elements such as Cu, As, Sb and Ag were high in the feed, which had direct impacts on the quality of the products and waste treatment.

The partitioning of elements, namely, the distribution ratios of elements in the products, can be manipulated by the operation parameters in industrial-scale processes, and the importance of obtaining their relationship is addressed. Although laboratory investigations as well as industrial statistical data regarding the element behavior in this process were reported [15,16], partitioning data either in a state far from equilibrium or only in a confined operation condition were disclosed, the relationship between the operation parameters and element behaviors is still unclear. It is suggested that the bath smelting system is close to thermodynamic equilibrium due to the high reaction temperature and intensified mass transfer rate in the agitated molten bath [17]. Moreover, SWINBOURNE and KHO [18] proposed that the behavior of minor elements in the flash smelting process mostly depends on their thermodynamic properties. Therefore, thermodynamic modeling is a promising solution and has drawn much attention in recent years [19]. WANG et al [20] built a multiphase equilibrium model for the copper converting process based on the minimum Gibbs free energy theory and simulated the behavior of As, Sb, Bi, Pb and Zn. YAMAGUCHI et al [21] simulated the Pb concentrate oxidative smelting process using HSC software, and the effect of the oxygen to feed ratio was analyzed. These works suggest that it is feasible to study the effect of operation parameters on element partitioning in the Pb−Bi concentrate bath smelting process using thermodynamic equilibrium method, which has less been reported up to date.

In this work, element partitioning in the Pb−Bi concentrate oxygen-rich bath smelting process was studied using thermodynamic equilibrium method. The influence of oxygen to feed ratio and sulfur dioxide partial pressure on the partitioning of Bi, Pb, As, Sb, Cu and Ag in the products was analyzed. The simulated results were compared with industrial data. This work provides a better understanding on element behaviors in the bath smelting process for a complex material, which could help to optimize industrial operations.

2 Equilibrium calculation method

Factsage software can be used to simulate the thermochemistry of processes, e.g. pyrometallurgical, hydrometallurgical, electro-metallurgical, and environmental studies [22]. The software enables the user to acquire an understanding of thermodynamics with the assistance of extensive data that are updated continuously [23−25]. The Equilib module in Factsage 6.2 was utilized in this work to simulate element equilibrium partitioning. For equilibrium calculations in this work, firstly, the masses of different components in the raw material were put in; secondly, proper thermodynamic databases were selected; next, activity coefficients absent in the databases were collected from the literature by critically reviewing; and finally, the boundary conditions for the thermodynamic simulation, such as the temperature, pressure and variables, were set. After the calculation, the mass and composition of all products were obtained, which can be used to calculate the element partitioning based on mass equilibrium.

2.1 Input of feed

The total mass of the solid feed was set to be 1000 kg. The solid feed was the mixture of Pb−Bi concentrate, flux and coal. The element and phase compositions of the feed are listed in Table 1, which originated from the assay of the feed of a smelter in Chenzhou, China [14]. According to the composition of the feed, this work was mainly focused on the partitioning of Bi, Pb, As, Sb, Cu and Ag in the oxidative smelting process. Pure oxygen was used as the oxidant and set as the second feed stream. The oxygen-to-solid feed ratio (OFR) is a key operation parameter in the industrial operation and its effect on element partitioning was studied by varying the oxygen input. In this work, the OFR was calculated with a feed mixture (moisture of 15 wt.%). The oxygen utilization efficiency was close to 100% in bath smelting systems [20].

Table 1 Element and phase compositions of solid feed

Component	Mass/kg	Element	Mass/kg	Mass fraction/%
PbS	493.9	Pb	427.8	42.78
ZnS	88.4	Fe	93.4	9.34
FeS	47.7	Cu	23.7	2.37
Cu_2S	29.7	Zn	59.3	5.93
As_2S_3	21.5	As	13.1	1.31
Sb_2S_3	1.8	Sb	1.3	0.13
Bi_2S_3	43.0	Bi	35.0	3.50
Ag_2S_3	3.1	Ca	17.5	1.75
Fe_3O_4	47.5	Mg	16.2	1.62
Fe_2O_3	41.1	Al	8.7	0.87
SiO_2	79.5	Si	37.2	3.72
CaO	24.5	Ag	2.1	0.21
Al_2O_3	16.4	S	136.6	13.66
MgO	26.9	H	1.67	0.17
H_2O	15.0	C*	20.0	2.00
C	20.0	O**	106.5	10.65
Total	1000	Total	1000	100

* From coal; ** From solid feed

2.2 Boundary conditions and activity coefficients

Four products were considered for the oxidative smelting process, namely, Pb−Bi metal alloy, oxidized slag, matte and dust. The typical Bi, Pb, As, Sb, Cu and Ag contents of the products and their partitioning were reported in the previous work [16]. According to the superimposed Pb−M−S−O (M=Bi, Cu, Sb, As) chemical potential diagram [26], the stable phase of Bi, Pb, As and Cu would be element, while that of Sb would be oxide (Sb_2O_3) in the oxidative smelting conditions (1250 °C, p_{O_2}=10^{-6}–10^{-5} kPa, and p_{SO_2}=10−100 kPa). The boundary conditions used for the simulation are listed in Table 2. The simulation was conducted at 1250 °C and atmosphere pressure. OFR was varied from 5.0 to 7.5 kmol/t to study the effect of oxygen partial pressure on the element partitioning. To investigate the influence of SO_2 partial pressure, the oxygen partial pressure in the system was fixed at $1\times10^{-5.25}$ kPa and then SO_2 partial pressure was changed from 10 to $1\times10^{1.9}$ kPa with an interval of $10^{2.1}$ kPa.

Table 2 Boundary conditions

Parameter	Value
Temperature/°C	1250
Total pressure/kPa	100
OFR/(kmol·t^{-1})	5.0−7.5
SO_2 partial pressure/kPa	10−$10^{1.9}$

The major difficulty in thermodynamic equilibrium calculations is selecting appropriate activity coefficients for the components in various phases [18]. However, some coefficients have not been experimentally measured and should be extrapolated from the literatures. The FToxide, FTmisc, and FACT databases in Factsage 6.2 were selected to provide thermodynamic data for the simulation. The FToxide database provided the activity coefficients in the slag phase; the FTmisc database provided the activity coefficients in the matte and metal phases; and the FACT database provided the thermodynamic parameters of the components in the gas phase. Note that the activity coefficients of Bi, Sb and Ag in the slag and matte phases were not available in these databases. Due to the lack of coefficient data in Pb-rich systems, literature data were critically reviewed and collected from Cu smelting systems, as listed in Table 3.

Table 3 Activity coefficients in matte and slag phases

Phase	Component	Activity coefficient formula	Ref.
Matte	Ag	$\lg\gamma=0.37+2830/T$	[27]
	Bi	$\lg\gamma=-2.03+4.44\times10^3/T$	[28]
	Sb	$\lg\gamma=-7539.2/T+6.3402$	[29]
Slag	$AgO_{0.5}$	$\lg\gamma=-750.31/T$	[30]
	$BiO_{1.5}$	$\lg\gamma=-502.76/T$	[30]
	$SbO_{1.5}$	$\lg\gamma=-485.16/T$	[30]

ZAKERI et al [27] measured the distribution of Ag in Cu−Cu_2S immiscible liquids using a double Knudsen cell configuration combined with a mass spectrometer. They proposed that the activity coefficient of Ag in molten matte could be described by $\lg\gamma=0.37+2830/T$. ZHONG and LYNCH [28] investigated the distribution of Bi between Cu_2S−FeS matte and blister Cu from 1493 to 1573 K. They disclosed that the activity of Bi was related to the sulfur deficit (SD) and Cu/Fe ratio in the matte phase. Under a sulfur deficit (SD=−0.02) and Cu/Fe ratio of 2.5, the activity coefficient can be described by $\lg\gamma=-2.03+4.44\times10^3/T$. LYNCH and ZHONG [29] studied the

activity coefficient of Sb in Cu_2S−FeS matte balanced with blister Cu. They found that temperature had little effect on the activity coefficient in the matte phase above 1530 K. The coefficient could be described by $\lg \gamma = -7539.2/T + 6.3402$. On the other hand, ROINE and JALKANEN [31] studied the effect of sulfur stoichiometry on the activity coefficients of As, Bi and Pb in homogeneous copper mattes at low iron concentrations. They disclosed that the SD had a strong influence on the activity coefficients of Sb and Bi in matte, while the impact of Fe content was less obvious. However, temperature dependency of the activity coefficients was not reported. According to the oxidative bath smelting condition and sulfur content in the oxidized slag (0.5−0.6 wt.%) [14], it could be speculated that the matte produced is a sulfur deficit matte entrained with metallic Pb, Bi, Sb, As or their sulfides. Therefore, the activity coefficients were collected from Refs. [28,29] in the sulfur deficit condition (SD=−0.02).

ROGHANI et al [30] tested the distribution of minor elements such as Bi, Sb and Ag between FeO_x−SiO_2−MgO slag and Cu_2S−FeS matte. The activity coefficients of $AgO_{0.5}$, $BiO_{1.5}$ and $SbO_{1.5}$ in the slag phase can be extrapolated from the distribution data as $\lg \gamma = -750.31/T$, $\lg \gamma = -502.76/T$, and $\lg \gamma = -485.16/T$, respectively. Procedure of the extrapolation can be referred from the supplementary file and Gibbs free energy needed for the extrapolation was obtained from HSC 6.0 [26].

The following compounds and solution phases were selected in Factsage for the simulation, and the missing activity coefficients of diluted Bi, Sb and Ag components in the matte and slag phases was added in the databases:

Gas phase (FACT): O_2(g), H_2(g), H_2O(g), CO(g), CO_2(g), S_2(g), SO_2(g), SO_3(g), Pb(g), Pb_2(g), PbO(g), PbS(g), PbSb(g), Bi(g), Bi_2(g), BiO(g), Bi_2O_3(g), BiS(g), Ag(g), Ag_2(g), AgS(g), Zn(g), ZnS(g), As(g), As_2(g), As_3(g), As_4(g), AsS(g), As_4O_6(g), Sb(g), Sb_2(g), Sb_4(g), SbS(g), Sb_4O_6(g), SbS(g), AsSb(g), As_2Sb_2(g), As_3Sb(g), $AsSb_3$(g), As_3SbO_6(g), $As_2Sb_2O_6$(g), $AsSb_3O_6$(g);

Slag phase (FToxide-SLAGA): Liquid slag oxide of Pb, Bi, Cu, As, Sb, Ag, Zn, Fe, Si, Ca, Al, Mg with diluted S;

Matte phase (FTmisc-MATT): Liquid matte of S−Pb−Bi−Cu−As−Sb−Ag−Zn−Fe with possilbe miscibility gap;

Metal phase (FTmisc-PbLQ): Liquid Pb with diluted Bi, Cu, As, Sb, Bi, Ag, Fe, Zn, S;

Spinel phase (FToxide-SPINA): MM'_2O_4 (M, M′=Fe, Mg, Al, Zn).

3 Results and discussion

3.1 Effect of oxygen partial pressure

One of the key operation parameters in the industrial bath smelting operations is the OFR, which will determine the oxygen partial pressure (p_{O_2}) in the system. In this work, different p_{O_2} values were achieved in the system by varying the OFR, as indicated by the dashed line in Fig. 1. Industrial OFRs were usually set at 140 $m^3(O_2)$/t (equal to 6.25 kmol/t) for the oxidative smelting process [16], and the industrial partitioning data are plotted in the figures for comparison. Figure 1 indicates that the OFR had strong impacts on the partitionings of Bi, Pb, As, Sb and Cu in the products, while its influence on the partitioning of Ag was weak. Partitionings of Bi, Pb, Sb, As and Cu in the gas and matte phases declined as the OFR increased from 5.0 to 6.3 kmol/t, while those in the metal and slag phases increased. Higher OFR decreased the quantity of matte, resulting in the increase of metal and slag. However, with a further increase of OFR, the rise of the slag partitionings of Pb, As, Sb and Cu was observed, accompanied by the decrease of metal partitioning. The simulated results suggest that the optimal OFR for the process was in the range from 6.3 to 6.8 kmol/t to maximize Bi, Pb, Cu and Ag partitioning in the metal phase. The formation of matte at low OFRs not only decreased direct metal recovery but also deteriorated furnace operation as the matte would form a high-melting point layer between the slag and metal phase [32]. On the other hand, an OFR higher than 6.8 kmol/t significantly raised the element partitioning in the slag phase, which decreased the direct recovery in the oxidative smelting process. Moreover, the increase of OFR would also lead to the expansion of the primary phase field of refractory spinels in the PbO−FeO_x−CaO−SiO_2 slag system, leading to the increase of the slag liquidus temperature [33]. Figure 2 shows the effect of p_{O_2} on the liquidus temperature of the oxidized slag. The composition of slag used for simulating the liquidus temperature

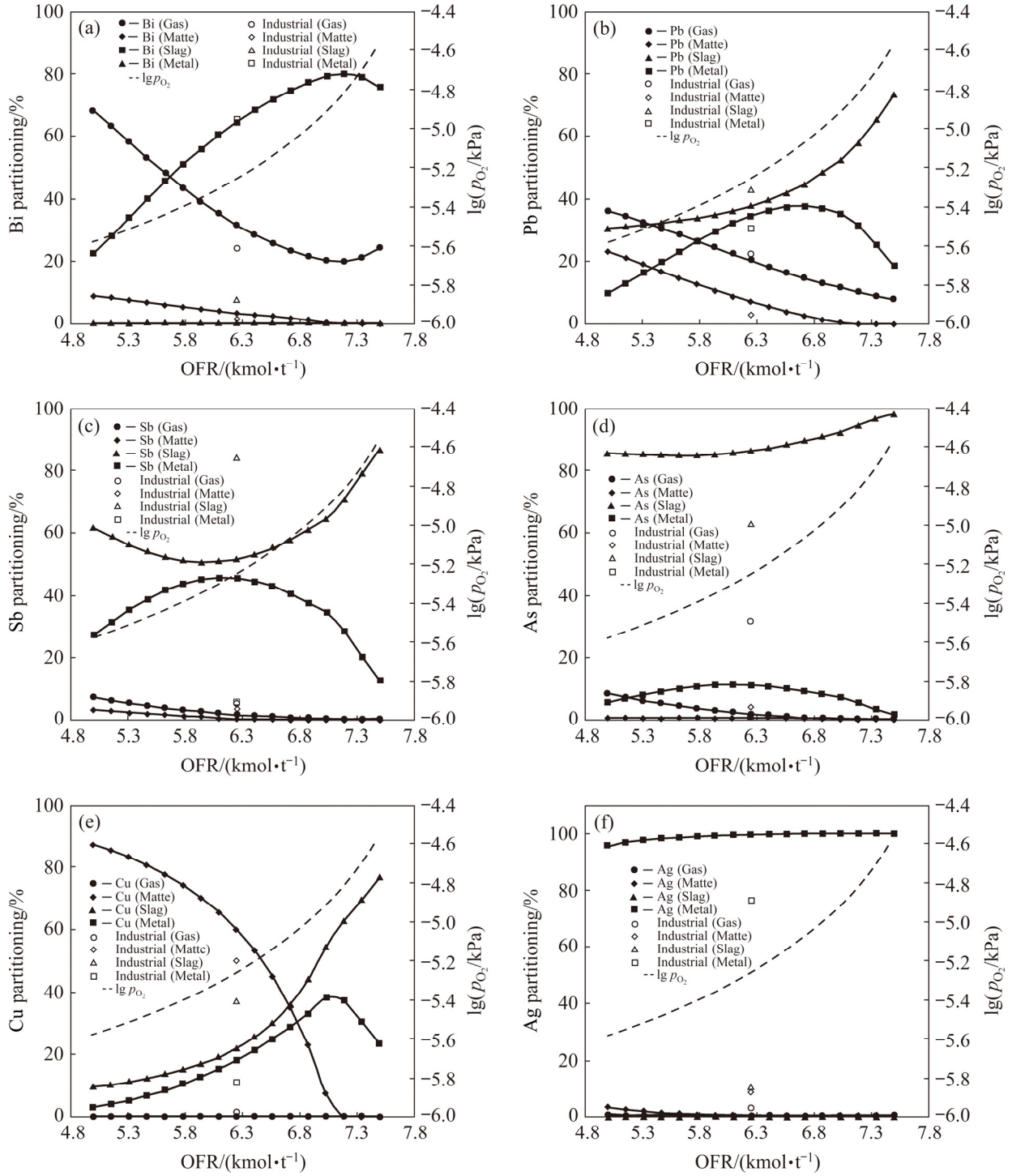

Fig. 1 Effect of oxygen partial pressure on element partitioning in oxidative smelting (1250 °C): (a) Bi; (b) Pb; (c) Sb; (d) As; (e) Cu; (f) Ag

is a PbO−ZnO−FeO−CaO−SiO_2 with 40 wt.% PbO and 14 wt.% ZnO, while FeO/SiO_2 and CaO/SiO_2 ratios are 1.3 and 0.3, respectively. This slag is typical in Pb pyrometallurgy and also used in this oxidizing Pb−Bi concentrate smelting process [14]. The results disclose that liquidus temperature of the slag would increase from 1488 K to 1515 K upon raising p_{O_2} from $1\times10^{-5.25}$ kPa to $1\times10^{-4.5}$ kPa (corresponding to an OFR increase from 6.25 to 7.5 kmol/t), which would greatly increase the risk of solid spinels formation. In fact, experimental investigation on the PbO−Fe_2O_3− SiO_2−CaO−ZnO system disclosed that the liquidus temperature exceeded 1300 °C at a high p_{O_2} (21 kPa) [33].

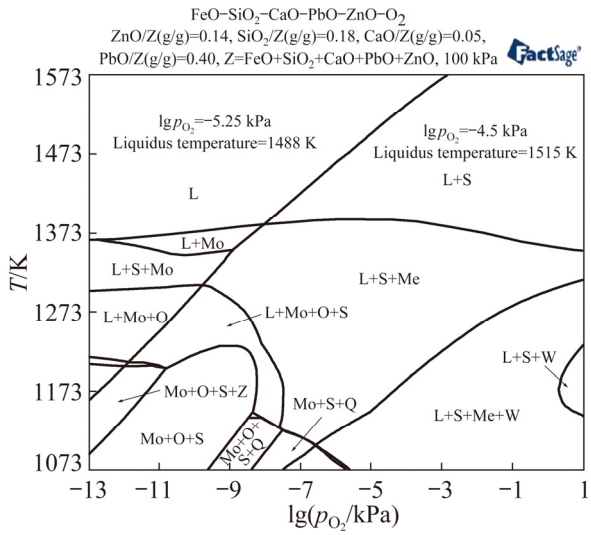

Fig. 2 Liquidus temperature of oxidized slag at different p_{O_2} values (L: Liquid slag; S: Spinel; Me: Melilite; Mo: Monoxide; W: Wollastonite; O: Olivine; Z: Zincite; Q: Quartz)

The industrial partitioning data are also plotted in Fig. 1. The data were obtained from 4.2 m^2 (cross section area) oxygen-rich side-blow bath smelting furnace (OSBF) using Pb−Bi concentrate as the raw material. Detailed structure and operation parameters of the OSBF were reported in the previous work [14]. As Fig. 1 shows, the simulated Pb and Bi partitionings coincided with the industrial data, and only the slag partitioning was slightly underestimated, which can be attributed to the metal/matte entrainment in the slag phase, as proven by the BSE analysis of the slag [14]. The simulated Cu and Ag partitionings were generally close to the industrial data, but the slag partitioning was also slightly underestimated. Because Ag would dissolve in the metal or matte phases, this result could also be ascribed to the metal/matte entrainment. The simulated As and Sb partitionings showed larger deviations: the slag partitioning of As and metal partitioning of Sb were overestimated, while the gas partitioning of As and the slag partitioning of Sb were underestimated. It could be speculated that there are two reasons for the deviation in the gas partitioning: firstly, the physical entrainment of feed in industrial operation was not considered in the thermodynamic simulation, and secondly, industrial smelting systems may not reach thermodynamic equilibrium due to the continuous charging of raw material, recycling of dust and discharging of products.

3.2 Effect of sulfur dioxide partial pressure

Due to the difficulty of measuring gas partial pressures in high-temperature smelting furnaces, the p_{O_2} value during industrial oxidative smelting is a topic of debate. YAZAWA [34] proposed that p_{SO_2} in the Pb concentrate oxidative smelting process was between 1 and 100 kPa [34]. CHENG et al [35] argued that mineral particles reacted on the surface of SO_2 bubbles generated in the oxidative smelting process, suggesting that the p_{SO_2} of the reaction should be 100 kPa. In this work, p_{SO_2}=50 kPa and $p_{O_2}=1\times10^{-5.25}$ kPa (OFR=6.25 kmol/t) were selected to plot the industrial data, and then the effect of p_{SO_2} (from 10 kPa to $1\times10^{2.1}$ kPa) on element partitioning was calculated, as shown in Fig. 3. The results indicate that increasing the p_{SO_2} greatly raised the gas partitioning of Bi and Pb and the matte partitioning of Cu, while the partitionings of As, Sb and Ag were not obviously influenced. Figure 4 shows the effect of p_{SO_2} on the Bi and Pb quantities and their phase distributions in the dust. It is shown that the increase of p_{SO_2} led to higher Bi and Pb deportment in the gas phase mainly in the form of sulfides, since the vapor pressures of Bi and Pb sulfides were lower than those of their oxides [36], which finally resulted in higher dust ratio. Because high dust ratio is an unfavorable problem in the industrial bath smelting process, the simulation results suggest that reducing the p_{SO_2} is a conducive way to decrease dust ratio.

3.3 Comparison of industrial and simulated results

Table 4 lists the Pb, Bi, Cu, As, Sb and Ag contents of the industrial and simulated samples. The simulated slag composition coincided with the industrial samples; however, compared with slag and metal, larger deviations were observed in the matte. The thermodynamic simulation over-estimated the Pb and Bi contents but under-estimated the Cu, As, Sb and Ag contents in the matte. However, these deviations showed little effect on Pb, Bi and Cu partitioning since the quantity of matte produced in the process was small. On the other hand, the partitionings of As, Sb and Ag were greatly influenced due to the relatively low content of these elements in the feed. It could be speculated that there were three reasons for these deviations. Firstly, the entrainment of metal/matte in the slag was not considered, which could lead to

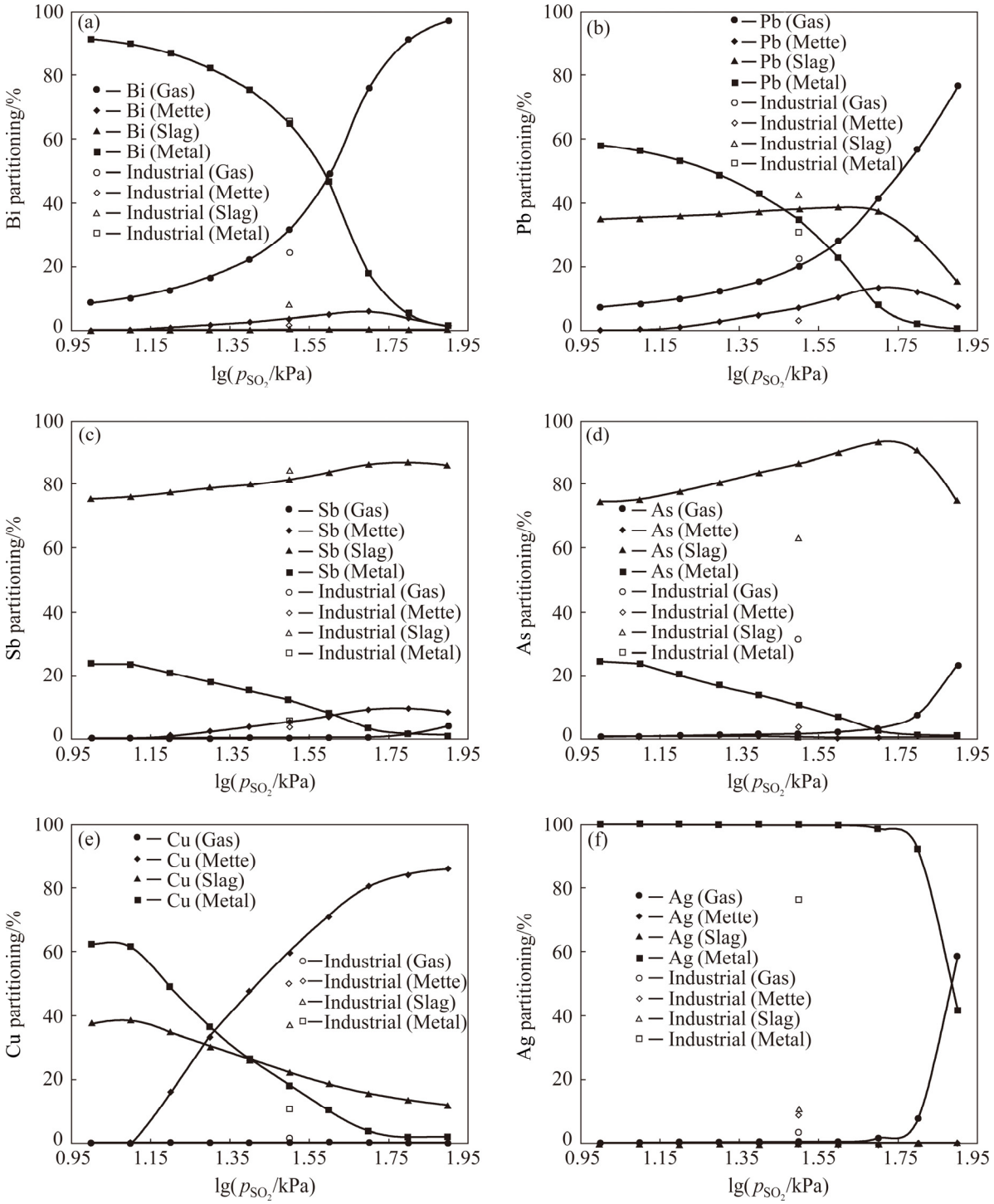

Fig. 3 Effect of SO_2 partial pressure on element partitioning: (a) Bi; (b) Pb; (c) Sb; (d) As; (e) Cu; (f) Ag

an underestimation of element partitioning in the slag. Secondly, there was the lack of precise thermo- dynamic data for Pb-rich smelting systems. The smelting bath for the process was a PbO−FeO_x−SiO_2−CaO−MgO−Al_2O_3 slag in which the activity coefficients have not been experimentally measured. As a result, the data for a simpler slag system in the FToxide database were used for calculations. Furthermore, although much work has been done on the As, Sb and Bi activity coefficients in Cu_2S−FeS matte [37,38], data for mattes rich in Pb and Bi were still unavailable. Thirdly, the differences between the thermodynamic equilibrium calculations and industrial conditions such as feeding, dust recycling and discharging operations should be considered based on detailed industrial

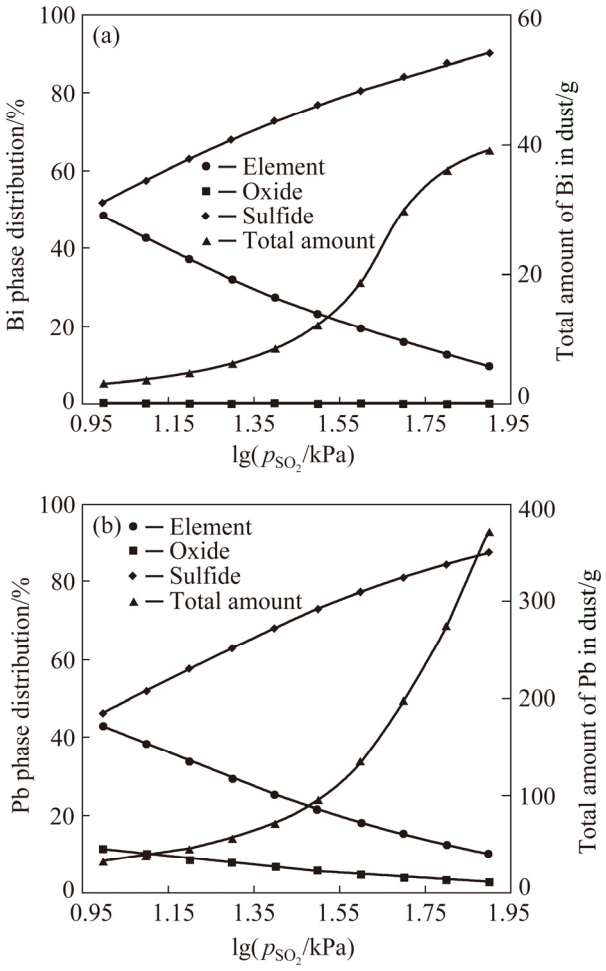

Fig. 4 Effect of p_{SO_2} on Bi (a) and Pb (b) quantity and phase in dust

Table 4 Comparison of industrial and simulated data (wt.%)

Source	Data	Pb	Bi	Cu	As	Sb	Ag
Slag	Simulated	33.36	0.00	1.18	2.24	0.13	0.00
	Industrial*	36.25	0.33	1.45	1.15	0.59	0.02
Metal	Simulated	81.55	12.52	2.64	0.73	0.30	1.129
	Industrial*	83.99	12.31	1.66	0.08	0.09	1.02
Matte	Simulated	53.32	2.29	28.19	0.23	0.02	0.02
	Industrial*	39.71	1.50	38.62	1.07	0.23	0.57

*Collected from Ref. [16]

process study. The deviations might be solved by combining thermodynamic simulation, hydrodynamics including kinetic studies and process calculation together. Meanwhile, more accurate thermodynamic data in Pb-rich systems needed to be developed.

4 Conclusions

(1) The element partitioning in the gas and matte phases decreased with increasing OFR, while the partitioning in the metal and slag phases increased. As the OFR increased from 5.0 to 7.5 m^3/t, the gas partitionings of Bi, Pb, Sb, and As decreased from 68.28%, 36.14%, 7.50% and 8.44% to 24.43%, 8.04%, 0.26% and 0.06%, respectively.

(2) The p_{SO_2} showed great impact on the gas partitionings of Bi and Pb and matte partitioning of Cu. As p_{SO_2} increased from 10 to $1\times10^{1.9}$ kPa, gas partitionings of Bi and Pb increased from 8.67% and 7.21% to 98.48% and 76.83%, respectively.

(3) The comparison between the simulated results and industrial data indicated that the simulated Pb and Bi partitionings coincided with the industrial data well, while those of Cu and Ag in the matte and metal deviated slightly. The simulated slag and metal compositions were consistent with the industrial samples, while a larger deviation was found in matte. The main reason for the deviation was the physical entrainment, the lack of accurate activity coefficients in the Pb-rich system, and the differences between thermodynamic calculations and industrial conditions.

Acknowledgments

The authors are grateful for the financial supports from the National Key R&D Program of China (2018YFC1901604), the Natural Science Foundation of Hunan Province, China (2018JJ3662), the China Scholarship Council (201706375005), the China Postdoctoral Science Foundation (2018M632988). The valuable discussion with Dr. Denis SHISHIN (PYROSEARCH, University of Queensland) is gratefully acknowledged.

References

[1] WOOD J, HOANG J, HUGHES S. Energy efficiency of the Outotec® ausmelt process for primary copper smelting [J]. JOM, 2017, 69: 1013−1020.

[2] CHEN Lin, YANG Tian-zu, BIN Shu, LIU Wei-feng, ZHANG Du-chao, BIN Wan-da, ZHANG Li. An efficient reactor for high-lead slag reduction process: Oxygen-rich side blow furnace [J]. JOM, 2014, 66: 1664−1669.

[3] CHEN Min, DAI Xi. Microscopic study of the phase transformation during the oxygen-enriched direct smelting of jamesonite concentrate [J]. JOM, 2018, 70: 41−46.

[4] KLEMETTINEN L, AVARMAA K, O'BRIEN H, TASKINEN P, JOKILAAKSO A. Behavior of tin and antimony in secondary copper smelting process [J]. Minerals, 2019, 9: 39−55.

[5] COURSOL P, MACKEY P J, KAPUSTA J P T, VALENCIA N C. Energy consumption in copper smelting: A new Asian horse in the race [J]. JOM, 2015, 67: 1066−1074.

[6] ZHANG Zhong-tang, LI Wei-feng, ZHAN Jing, LI Gui, ZHAO Zhen-bo. Thermodynamic analysis of the bottom-blown direct reduction of lead sulfate with carbon [J]. Journal of Thermal Analysis and Calorimetry, 2019, 136: 2397−2407.

[7] KAPUSTA J P T. Sonic injection in sulphide bath smelting: An update [J]. Journal of the Southern African Institute of Mining and Metallurgy, 2018, 118: 1131−1139.

[8] LOTFIAN S, AHMED H, UMEKI K, SAMUELSSON C. Conversion characteristics of alternative reducing agents for the bath smelting processes in an oxidizing atmosphere [J]. Journal of Sustainable Metallurgy, 2019, 5: 230−239.

[9] SUKHOMLINOV D, AVARMAA K, VIRTANEN O, TASKINEN P, JOKILAAKSO A. Slag-copper equilibria of selected trace elements in black-copper smelting. Part II: Trace element distributions [J]. Mineral Processing and Extractive Metallurgy Review, 2020, 41: 171−177.

[10] UPHAM D C, AGARWAL V, KHECHFE A, SNODGRASS Z R, GORDON M J, METIU H, MCFARLAND E W. Catalytic molten metals for the direct conversion of methane to hydrogen and separable carbon [J]. Science, 2017, 358: 917.

[11] JIANG Qing-mei, ZHANG Miao-rong, LUO Li-qiang, PAN Ge-bo. Electrosynthesis of bismuth nanodendrites/gallium nitride electrode for non-enzymatic hydrogen peroxide detection [J]. Talanta, 2017, 171: 250−254.

[12] ZHANG Du-chao, ZHANG Xin-wang, YANG Tian-zu, WEN Jian-feng, LIU Wei-feng, CHEN Lin, RAO Shuai, XIAO Qing-kai, HAO Zhan-dong. Reduction smelting on bismuth oxide residue in FeO−SiO_2−CaO ternary slag system [J]. Journal of Central South University, 2016, 23: 1326−1331.

[13] YANG Tian-zu, LI Jun, LIU Wei-feng, CHEN Lin, BIN Wan-da. Development of bismuth smelting technology in China [C]//JIANG Tao, HWANG J Y, MACKEY P J, YUCEL O, ZHOU Gui-feng. TMS Annual Meeting. San Antonio, 2013: 631−642.

[14] CHEN Lin, HAO Zhan-dong, YANG Tian-zu, XIAO Hui, LIU Wei-feng, ZHANG Du-chao, BIN Shu, BIN Wan-da. An efficient technology for smelting low grade bismuth−lead concentrate: Oxygen-rich side blow process [J]. JOM, 2015, 67: 1997−2004.

[15] YANG Tian-zu, XIAO Hui, CHEN Lin, CHEN Wei, LIU Wei-feng, ZHANG Du-chao. Elements behavior in bath smelting of low-grade lead-bismuth material [J]. The Chinese Journal of Nonferrous Metals, 2018, 28: 1883−1892. (in Chinese)

[16] YANG Tian-zu, XIAO Hui, CHEN Lin, CHEN Wei, LIU Wei-feng, ZHANG Du-chao. Element distribution in the oxygen-rich side-blow bath smelting of a low-grade bismuth−lead concentrate [J]. JOM, 2018, 70: 1005−1010.

[17] LENNARTSSON A, ENGSTRÖM F, BJÖRKMAN B, SAMUELSSON C. Development of a model for copper converting [J]. Canadian Metallurgical Quarterly, 2013, 52: 422−429.

[18] SWINBOURNE D R, KHO T S. Computational thermodynamics modeling of minor element distributions during copper flash converting [J]. Metallurgical and Materials Transactions B, 2012, 43: 823−829.

[19] KUANG Shi-bo, LI Zhao-yang, YU Ai-bing. Review on modeling and simulation of blast furnace [J]. Steel Research International, 2018, 89: 1700071.

[20] WANG Qin-meng, GUO Xue-yi, WANG Song-song, LIAO Li-le, TIAN Qing-hua. Multiphase equilibrium modeling of oxygen bottom-blown copper smelting process [J]. Transactions of Nonferrous Metals Society of China, 2017, 27: 2503−2511.

[21] YAMAGUCHI K, SWINBOURNE D R, YAZAWA A. Behaviour of minor species during oxidation smelting of lead concentrate [C]//KONGOLI F, ITAGAKI K, YAMAUCHI C. Yazawa International Symposium on Metallurgical and Materials Processing. Fujisawa: Minerals, Metal & Materials Society, 2005: 1231−1246.

[22] BALE C W, BÉLISLE E, CHARTRAND P, DECTEROV S A, ERIKSSON G, GHERIBI A E, HACK K, JUNG I H, KANG Y B, MELANÇON J, PELTON A D, PETERSEN S, ROBELIN C, SANGSTER J, SPENCER P, van ENDE M A. FactSage thermochemical software and databases, 2010−2016 [J]. Calphad−Computer Coupling of Phase Diagrams and Thermochemistry, 2016, 54: 35−53.

[23] SHISHIN D, HIDAYAT T, CHEN Jiang, HAYES P C, JAK E. Combined experimental and thermodynamic modelling investigation of the distribution of antimony and tin between phases in the Cu−Fe−O−S−Si system [J]. Calphad−Computer Coupling of Phase Diagrams and Thermochemistry, 2019, 65: 16−24.

[24] SHEVCHENKO M, NICOL S, HAYES P C, JAK E. Experimental liquidus studies of the Pb−Cu−Si−O system in equilibrium with metallic Pb−Cu alloys [J]. Metallurgical and Materials Transactions B, 2019, 49: 1690−1698.

[25] HIDAYAT T, CHEN Jiang, HAYES P C, JAK E. Distributions of Ag, Bi, and Sb as minor elements between iron-silicate slag and copper in equilibrium with tridymite in the Cu−Fe−O−Si system at T=1250 °C and 1300 °C (1523 K and 1573 K) [J]. Metallurgical and Materials Transactions B, 2019, 50: 229−241.

[26] ROINE A. HSC chemistry for Windows 6.0 [M]. Pori, Finland: Outotec Research, 2019.

[27] ZAKERI A, HINO M, ITAGAKI K. Activity of silver in molten copper sulfide saturated with copper [J]. Materials Transactions, JIM, 1998, 39: 1101−1107.

[28] ZHONG T, LYNCH D C. Henrian activity coefficient of Bi in Cu−Fe mattes and white metal [J]. Canadian Metallurgical Quarterly, 2000, 39: 23−36.

[29] LYNCH D C, ZHONG T. Volatilization and activity coefficient of Sb in Cu−Fe mattes and white metal [J]. Canadian Metallurgical Quarterly, 2005, 44: 409−420.

[30] ROGHANI G, TAKEDA Y, ITAGAKI K. Phase equilibrium and minor element distribution between FeO_x−SiO_2−MgO-based slag and Cu_2S−FeS matte at 1573 K under high partial

pressures of SO_2 [J]. Metallurgical and Materials Transactions B, 2000, 31: 705−712.

[31] ROINE A, JALKANEN H. Activities of As, Sb, Bi, and Pb in copper mattes [J]. Metallurgical and Materials Transactions B, 1985, 16: 129−141.

[32] LI Yun, YANG Sheng-hai, TASKINEN P, HE Jing, CHEN Yong-ming, TANG Chao-bo, WANG Yue-jun, JOKILAAKSO A. Spent lead-acid battery recycling via reductive sulfur-fixing smelting and its reaction mechanism in the $PbSO_4$−Fe_3O_4−Na_2CO_3−C system [J]. JOM, 2019, 71: 2368−2379.

[33] JAK E, HAYES P C. Experimental liquidus in the PbO−ZnO−"Fe_2O_3"−($CaO+SiO_2$) system in air, with CaO/SiO_2=0.35 and $PbO/(CaO+SiO_2)$=3.2 [J]. Metallurgical and Materials Transactions B, 2002, 33: 851−863.

[34] YAZAWA A. Thermodynamic evaluations of extractive metallurgical processes [J]. Metallurgical Transactions B, 1979, 10: 307−321.

[35] CHENG Xiang-feng, CUI Zhi-xiang, CONTRERAS L, CHEN Mao, NGUYEN A, ZHAO Bao-jun. Matte entrainment by SO_2 bubbles in copper smelting slag [J]. JOM, 2019, 71: 1897−1903.

[36] STEINACKER S R, ANTREKOWITSCH J. Aspects concerning the formation of flue dust in the primary copper industry [J]. Matéria (Rio de Janeiro), 2018, 23: 12143.

[37] SHISHIN D, HIDAYAT T, CHEN Jiang, HAYES P C, JAK E. Integrated experimental study and thermodynamic modelling of the distribution of arsenic between phases in the Cu−Fe−O−S−Si system [J]. The Journal of Chemical Thermodynamics, 2019, 135: 175−182.

[38] AVARMAA K, JOHTO H, TASKINEN P. Distribution of precious metals (Ag, Au, Pd, Pt, and Rh) between copper matte and iron silicate slag [J]. Metallurgical and Materials Transactions B, 2016, 47: 244−255.

复杂铅铋精矿氧化熔池熔炼过程的热力学模拟

陈 霖[1,2]，陈 鹏[1,2]，张杜超[1,2]，刘伟锋[1,2]，杨天足[1,2]

1. 中南大学 冶金与环境学院，长沙 410083；
2. 中南大学 难冶有色金属资源高效利用国家工程实验室，长沙 410083

摘 要：采用热力学平衡模拟方法研究复杂铅铋精矿富氧熔池熔炼过程中的元素分配行为，分析氧料比(OFR)和硫分压(p_{SO_2})对 Bi、Pb、As、Sb、Cu 和 Ag 分配行为的影响，并对比模拟计算结果与工业数据。结果表明，该过程中 OFR 在 6.3~6.8 kmol/t 之间有利于最大化 Bi、Pb、Cu 和 Ag 在金属相中的分配，进一步增加 OFR 将导致金属相分配率下降和渣液化温度提高。此外，高 p_{SO_2}将导致 Bi 和 Pb 以硫化物形式大量分配至烟尘相，这表明低 p_{SO_2}有利于降低过程烟尘率。

关键词：复杂铅铋精矿；富氧熔池熔炼；多相平衡模拟；元素分配；过程参数优化

(Edited by Bing YANG)